PCCP

RSC Publishing

PAPER

View Article Online
View Journal | View Issue

Cite this: *Phys. Chem. Chem. Phys.*, 2013, **15**, 14290

Improved cathode for high efficient microbial-catalyzed reduction in microbial electrosynthesis cells

Huarong Nie,†[a] Tian Zhang,†[b] Mengmeng Cui,[a] Haiyun Lu,[a] Derek R. Lovley*[b] and Thomas P. Russell*[a]

Received 27th June 2013,
Accepted 11th July 2013

DOI: 10.1039/c3cp52697f

www.rsc.org/pccp

Microbial electrosynthesis cells (MECs) are devices wherein microorganisms can electrochemically interact with electrodes, directly donating or accepting electrons from electrode surfaces. Here, we developed a novel cathode by using nickel nanowires anchored to graphite for the improvement of microbial-catalyzed reduction in MEC cathode chamber. This porous nickel-nanowire-network-coated graphite electrode increased the interfacial area and interfacial interactions between the cathode surface and the microbial biofilm. A 2.3 fold increase in bio-reduction rate over the untreated graphite was observed. Around 282 mM day^{-1} m^{-2} of acetate resulting from the bio-reduction of carbon dioxide by *Sporomusa* was produced with 82 ± 14% of the electrons consumed being recovered in acetate.

Introduction

Microbial fuel cells (MFCs) are devices wherein microorganisms can electrochemically interact with electrodes and directly transfer electrons to electrodes.[1,2] Most studies have indicated that electricity can be produced from the waste organic matters and renewable biomass by microorganisms directly donating electrons to electrode surface.[1,3] Intense investigation on MFCs is still under way for the optimization of anode for high efficiency power generation.[4,5] In fact, one more interesting aspect is that microorganisms can also directly accept electrons from an electrode that is at enough low potential for chemical conversion in microbial electrosynthesis cells (MECs).[6] The initial and insightful studies of microbe–cathode interactions have provided guidance to the field.[7,8] Further empirical studies on this microbial-catalyzed reduction in MECs include the cathode design for high efficient chemical conversion from the improved electron transfer.[8]

Developments of anodic materials in MFCs demonstrated a porous surface of the electrode, as opposed to a planar electrode surface, contributed to a higher specific surface area to interface with bacteria and enhanced electron-exchange at the electrode surface.[5,9] Similar ideas have been put forth for the design of cathode in MECs to improve the microbial-catalyzed reduction. Recently, we have shown enhanced microbial reduction of carbon dioxide to acetate with the use of a modified carbon cloth cathode by increasing the surface area, anchoring positively charged groups, and introducing metallic nanoparticles with electrocatalytic activity.[8] In particular, for nickel nanoparticles deposited on carbon cloth cathode, 136 ± 33 mM day^{-1} m^{-2} of acetic acid, almost 4 times larger than that achieved with the plain carbon cloth, was generated by acetogenic bacteria, *Sporomusa* while maintaining low cost. However, due to the light weight, carbon cloth cathode cannot always be used efficiently and stably in an agitated media, which represents a serious limitation.

Initial proof-of-concept studies reported approximately 123 mM day^{-1} m^{-2} of acetate was produced with a steady consumption of current over time by *Sporomusa* with a graphite stick cathode as the sole electron donor.[7] Therefore, designing a graphite electrode with tailored surface functionality to facilitate the microbe colonization is desirable to develop highly efficient microbial electrodes. In comparison to nickel nanoparticles, the coating of nickel nanowires on graphite takes advantage of their unique properties, such as higher surface area and porous structure. However, unlike electrodeposition, sputter coating or physical vapor deposition of metal particles, it is a greater challenge to obtain a stable coating of the nickel nanowires on a planar graphite surface. Here, we approached this issue by using a nickel nanoparticle coated graphite as high thermal energy generator in a microwave to weld the Ni nanowire network that were deposited on

[a] *Department of Polymer Science and Engineering, University of Massachusetts, Amherst, Massachusetts 01003, USA. E-mail: russell@mail.pse.umass.edu; Fax: +1-413-577-1510; Tel: +1-413-545-2680*

[b] *Department of Microbiology, University of Massachusetts, Amherst, Massachusetts 01003, USA. E-mail: dlovley@microbio.umass.edu; Fax: +1-413-545-1578; Tel: +1-413-545-9651*

† Equally contributed to this work.

top of the nanoparticle coated graphite substrate. The modified electrodes were then monitored for their performance in MECs by *Sporomusa*-catalyzed reduction of carbon dioxide to acetate.

Results and discussion

Fig. 1A shows the SEM images of nickel nanowires network clearly linking each other and forming a porous network with the average diameter of the nanowires being ~160 nm. These nanowires appear as an assembly of nearly spherical nanoparticles (Insert of Fig. 1A). It is apparent that nickel nanowires were formed exclusively and no spherical nanoparticles or other morphologies were obtained.

Microwave irradiation is a powerful tool for heating. Graphite displays strong microwave absorption because of its low resistance, being able to transmit high thermal energy to supported materials.[10] However, due to the heating produced by microwave irradiation greatly depends on the size, shape and structure of the absorber,[11,12] the microwave heating of bulk graphite was not able to weld nickel nanowires on its surface. It has been suggested that most metals and some metal oxides in a powder form can be heated very efficiently by coupling to the electric and/or the magnetic component of the microwave field.[13] Therefore, a thin layer of nickel nanoparticles was electrodeposited on graphite surface to enhance the microwave heating before nickel nanowires could coat the surface (Fig. 1B). In striking contrast, the fusion of nickel nanowires at the graphite interface was observed after 3 minutes of microwave irradiation (Fig. 1C). The fusion of nickel nanowires increased with the irradiation time and that the nickel nanowires in contact with the graphite substrate were almost completely melted onto the surface after microwave irradiation for 5 minutes (Fig. 1D). As a result, the interior welded nickel nanowires served as the tether for the stable adhesion of the nickel nanowire network on the graphite surface. As shown in the insert of Fig. 1D, the morphology of the nickel nanowires on the top layer of the network was maintained without significant fusion, thus a porous nickel nanowires layer was formed on the graphite electrode. This conductive nickel nanowire network with microscale pores is expected to provide strong interaction with microbial biofilms.

During the microwave irradiation the nickel nanowires underwent a change in the structure, as evidenced by X-ray diffraction (XRD, Fig. 2). Reflections at 2θ values of 45.39°, 52.79°, and 78.24° are seen for the pristine nickel nanowires, which can be assigned to the (111), (200), and (220) planes, respectively, of face-centered cubic nickel. No obvious reflections attributable to the presence of nickel oxide were observed, indicating that the presence of an oxide layer on the nanowire surface was negligible. After microwave irradiation, the XRD patterns of the composite samples showed additional reflections at 43.31°, 60.69°, and 77.22° corresponding to (200), (220), and (311) planes of nickel oxide. By increasing the microwave irradiation time from 3 to 5 minutes, the relative amount of nickel oxide to nickel did not change, since the nickel oxide coating on the surface protected the interior nickel nanowires. Interestingly, the point of zero-charge (PZC) for the nickel oxide surface occurs at a pH ~ 8.45 near room temperature.[14] Here, the pH value of the working environment of the cathode is around 7. This means that the surface of nickel oxide should be positively charged with the generation of acetic acid in a microbial electrosynthesis media,[15] which may promote an electrostatic interaction with the negatively charged bacteria.

To investigate the electrochemical behavior of the Ni modified graphite as a cathode for the synthesis of acetate in MECs, cyclic voltammetry (CV) was performed in a *Sporomusa* culture. No redox peaks were detected on the current–potential curve (Fig. 3) with the Ni modified graphite electrode and untreated graphite electrode, indicating no soluble species were excreted by bacteria as electron shuttles involved in the

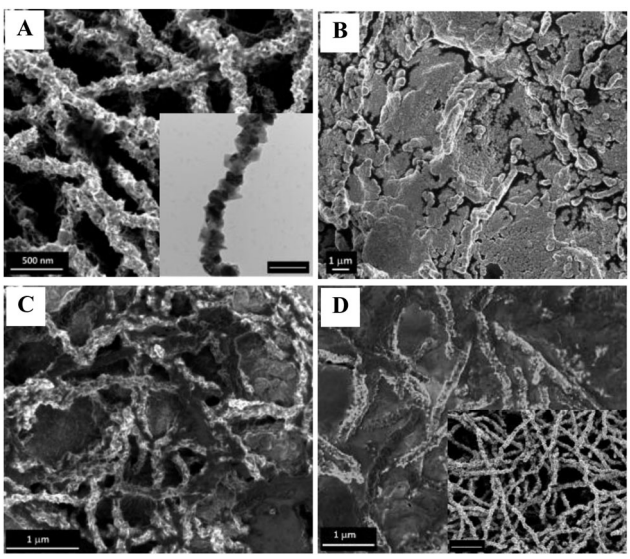

Fig. 1 SEM image of (A) original nickel nanowire network, and the insert is TEM micrograph of nickel nanowires (The scale bar is 200 nm), (B) nickel nanoparticles coated graphite, (C,D) nickel nanowires on nickel nanoparticle-coated graphite with microwave radiation for 3 min and 5 min. The insert is the final morphology of nickel nanowire coated graphite electrode (The scale bar is 1 μm).

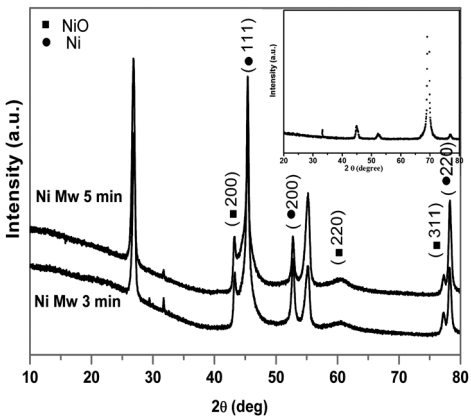

Fig. 2 X-ray diffraction pattern of nickel nanowire-coated graphite electrodes resulting from microwave irradiation for different time. The insert is X-ray diffraction of nickel nanowires on silicon wafer.

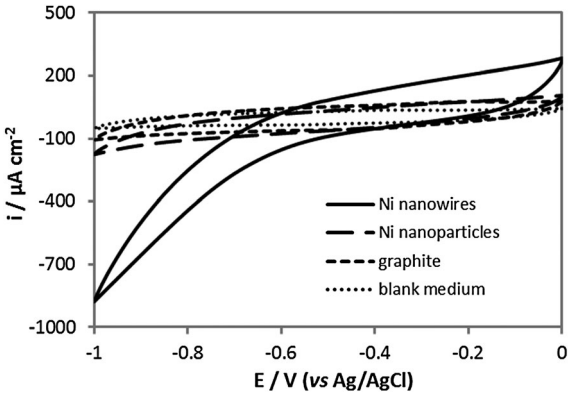

Fig. 3 The cyclic voltammograms obtained on a nickel nanowire-coated graphite electrode, Ni nanoparticle-coated graphite electrode, untreated graphite in *Sporomusa* culture, and untreated graphite in blank medium omitting carbon dioxide. Scanning rate: 100 mV s^{-1}.

electron transport processes. Apparently, nickel nanowire-coated graphite exhibited a higher cathodic current density (-0.89 mA cm^{-2} Fig. 4A) than the untreated graphite (-0.1 mA cm^{-2}) and the nickel nanoparticle-coated graphite (-0.17 mA cm^{-2}). The current draw at -600 mV *vs.* Ag/AgCl with Ni nanowires modified graphite electrode during a negative scan is $\sim$1.6 fold higher than with untreated graphite electrode (Fig. 3). There is no obvious difference in the current–potential curves between the Ni nanoparticle-coated graphite electrode and the untreated graphite electrode. This translates into an increased electron-exchange capacity resulting from the porous structure of the nickel nanowire network on the graphite (Fig. 1D), opening a route to enhance microbially catalyzed reaction in MECs.

Surface properties, such as topography and surface charge, can affect cell adhesion, growth, and metabolism in MECs. Fig. 4(A–C) shows the morphology of bacteria on the nickel nanowire-modified graphite cathode. It is seen that a substantial amount of *Sporomusa* accumulated on the electrode surface to form a continuous biofilm. The conductive nanowire network effectively tethers the bacteria to the electrode surface and promotes the stabilization of a biofilm.[5,9,16] This behavior is not observed on the nickel nanoparticle-coated graphite cathode (Fig. 4D) or the untreated graphite sticks.[7] The possible reason is that the porous layer of nickel nanowires created a rougher surface on modified graphite than that on nickel particles deposited graphite, indicates that the porous nature of the nickel nanowire-modified surface has a roughness and porosity on the right length scale to effectively entrap the microbes and provide a substantially enhanced surface area with which the microbes can interact (Fig. 4A and C). It is calculated that the surface area of nickel nanowire networks coated graphite is more than 50 times larger than that of original graphite based on the density of wires and the diameter of the nanowires. *Sporomusa* belongs to the class of gram-negative micro-organisms having a negative outer surface charge.[17] The positively charged surface of nickel nanowires may also accounts for the high cell density on modified cathode.[8,18] The increased biofilm-cathode interfacial surface area and the interaction between the cathode surface and the microbial biofilm will also facilitate the enhanced microbial-catalyzed reduction in MECs.

The performance of the nickel nanowire-coated graphite cathodes were tested using the *Sporomusa* catalyzed reduction of carbon dioxide to acetate in a dual chamber MECs. The reduction reaction rate was evaluated by the time-dependent production of acetate. As a control, the performance of nickel nanoparticles coated graphite electrodes was also measured. For the nickel nanowire-coated graphite without microwave treatment, the nanowires had poor

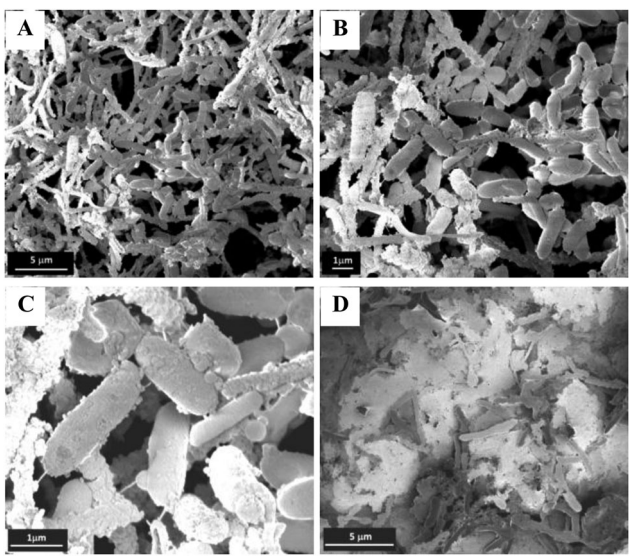

Fig. 4 SEM micrographs of *Sporomusa* cells adhered (A–C) on nickel nanowire-coated graphite electrode and (D) on nickel nanoparticle-coated graphite.

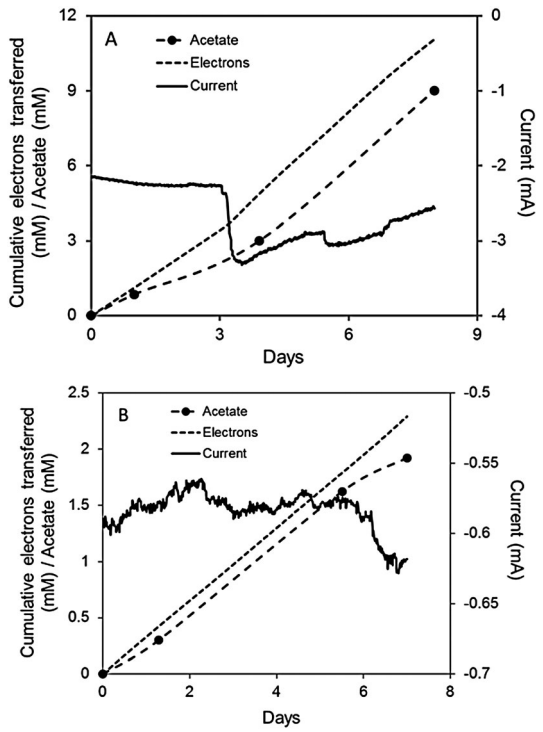

Fig. 5 Electron consumption, acetate and current production over time with different cathodes: (A) nickel nanowire-coated graphite cathode and (B) nickel nanoparticle-coated graphite cathode.

adhesion to the graphite surface in the agitated solution and peeled off. After four days, almost all of nickel nanowires detached and were dispersed in the medium. In striking contrast, after nickel nanowires were welded to graphite by microwave irradiation, no nickel nanowires were found in the suspension in the cathode chamber. As shown in Fig. 5A, about 282 mM day^{-1} m^{-2} of acetate was generated with the nickel nanowire-coated graphite cathode, *i.e.* nearly a 2.3-fold increase in bio-reduction rate was achieved in comparison to the untreated graphite stick.[7] Electron recovery in the acetate remained high with 82 ± 14% of the electrons consumed being recovered in acetate. The rate of acetate production corresponded to the current drawn at −600 mV on the different cathodes. The rate of acetate production *via* reduction reaction with the nickel nanoparticle-coated graphite was 76 mM day^{-1} m^{-2} with 84 ± 9% of the electrons consumed being recovered in acetate (Fig. 5B). This means that the nickel nanowire-modified graphite afforded enhanced microbial catalyzed reduction of carbon dioxide, due in large part to the superior surface topography resulting from the nature of the porous nanowire layer. The porous nickel nanowires on the graphite cathode improved the interaction between the cathode surface and the microbial biofilm, which accounts for the higher value of acetate production.

Experimental

Materials

Nickel acetate tetrahydrate, ethylene glycol were purchased from Sigma. Hydrazine monohydrate was purchased from Fisher Scientific (99–100%). All chemicals were used without further purification. *Sporomusa* ovata (DSM 2662) was obtained from Deutsche Sammlung Mikroorganismen (DSM) und Zellkulturen and routinely grown in DSM medium 311 (omitting betaine, fructose, casitone, and resazurin) with hydrogen as the electron donor (H_2–CO_2 [80 : 20]) at 30 °C under strict anaerobic conditions as previously described.[7,8]

Synthesis of nickel nanowires

Nickel nanowires were synthesized as described in the literature.[19] Briefly, 1 M aqueous solution of nickel chloride was prepared and the required volume of this solution was added to 10 mL of ethylene glycol in a glass bottle of 20 mL capacity to get a 10 mM solution of Ni^{2+}. The mixture was heated on a hot plate to 120 °C. Approximately 0.5 mL of hydrazine hydrate solution was added rapidly into the hot solution with a micropipette. Nickel nanowires were separated by a magnet and washed thoroughly with distilled water to remove excess hydrazine and solvent. Nickel nanowires were suspended in water before use.

Fabrication of cathode

First, graphite was pre-coated with a thin layer of nickel nanoparticles by electro-deposition. In this process, standard nickel deposition solution containing 380 g L^{-1} $NiSO_4 \cdot 6H_2O$ and 25 g L^{-1} H_3BO_3 was prepared. The electro-deposition was conducted using an Agilent E3612A DC power supply, with a two-electrode cell consisting of a graphite working electrode and a platinum foil counter electrode. Nickel nanoparticle films were deposited at 3 V for 60 s. The deposited electrode was washed with deionized water several times, then dried at room temperature. Subsequently, nickel nanowires suspension were drop cast onto the nickel nanoparticle-coated electrodes. After drying, the electrodes were placed in a microwave oven (GE Appliance, 1000 Watt) and irradiated for 1–5 minutes.

Microbial-catalyzed reduction reaction and cyclic voltammetry

Each cathode material was tested at least two times at 25 °C in a three-electrode, dual-chambered system, with *Sporomusa* grown in the cathode chamber as previously described.[7,8] The graphite cathode (40 cm^2; Mersen, Greenville, MI) and graphite stick anode (65 cm^2; Mersen, Greenville, MI) are suspended in 200 mL of media in two chambers which are separated by a Nafion 117 cation-exchange membrane (Electrolytica, Amherst, NY). The anode chamber was continually bubbled with N_2–CO_2 (80 : 20). The cathode was poised with a potentiostat (ECM8, Gamry Instruments, PA, USA) at −600 mV (*versus* Ag/AgCl). Hydrogen-grown cultures of *Sporomusa* were established in the cathode chamber in a medium that described above, and hydrogen containing gas mix N_2–CO_2–H_2 (83 : 10 : 7) was used as additional electron donor to gas out the cathode chamber for biofilm growth. The cathode gas mix was switched to N_2–CO_2 (80 : 20) after several fresh medium swaps. As previously described, there was no significant H_2 production with any of the cathode materials.[7]

The working electrodes (15 mm × 10 mm × 1 mm, in size) in the voltammetric measurements were prepared the same way as described above. The potentiostat (Model 2053, AMEL Instruments, Milano, Italy) was computer-operated Echem version 2.010 (eDAQ, Colorado Springs, CO, USA) and was interfaced to the potentiostat with a Powerlab data acquisition system (Model 4SP, ADInstruments, Colorado Springs, CO, USA). CV was performed from 0–1000 mV *vs.* the Ag/AgCl reference electrode at a scan rate of 100 mV s^{-1}. The solution is purged with oxygen-free N_2 for 25 min before electrochemical measurements.

Characterization

The morphology was studied with FESEM (FEI Magellon 400, Japan) and high-resolution transmission electron microscopy (JEM-2000FX, JEOL, Japan). Acetate was measured *via* high performance liquid chromatography (HPLC) as previously described.[7,8] X-ray diffraction (XRD) experiments were performed in a Shimadzu XRD-6000 X-ray powder diffractometer with Cu Kα (λ = 0.154 nm) radiation at a generator voltage of 45 kV and a current of 40 mA.

Conclusions

In summary, we developed a novel cathode for highly efficient microbial-catalyzed reduction in MECs by applying nickel nanoparticle-coated graphite as the thermal seed to weld nickel nanowire networks on graphite surface in a microwave field. The nickel nanowires produced a porous mesh on the graphite

and positively-charged surface, which enhanced the interactions between the microbial biofilm and the electrode surface, leading to an environment that was conducive to microbial colonization. The reduction reaction rate of carbon dioxide to acetate achieved by this modified graphite cathode were 1.3 times faster than that of the untreated graphite with 82 ± 14% of the electrons consumed being recovered in acetate. However, for a nickel nanoparticle-coated graphite cathode, no obvious enhancement in the production of acetate was observed. The high production of acetate obtained by this cathode in MECs will boost the rapid development of microbial-catalyzed reductions in terms of both fundamental research and applications.

Acknowledgements

The microbial research was supported by the Office of Science (BER), US Department of Energy, Cooperative agreement No. DE-FC02-ER63446 and Grant No. DE-FG02-07ER64367. Research on the modification of the electrode surface was supported by the Department of Energy Office of Basic Energy Science through contract DE-FG02-96ER45612.

References

1 (*a*) B. E. Logan and K. Rabaey, *Science*, 2012, **337**, 686; (*b*) B. E. Logan and M. Elimelech, *Nature*, 2012, **488**, 313; (*c*) D. R. Bond, D. E. Holmes, L. M. Tender and D. R. Lovley, *Science*, 2002, **295**(5554), 483; (*d*) G. Reguera, K. D. McCarthy, T. Mehta, J. S. Nicoll, M. T. Tuominen and D. R. Lovley, *Nature*, 2005, **435**(7045), 1098; (*e*) L. M. Tender, C. E. Reimers, H. A. Stecher, D. E. Holmes, D. R. Bond, D. A. Lowy, K. Pilobello, S. J. Fertig and D. R. Lovley, *Nat. Biotechnol.*, 2002, **20**, 821.

2 (*a*) Y. A. Gorby, *et al.*, *Proc. Natl. Acad. Sci. USA*, 2006, **103**, 11358; (*b*) J. P. Busalmen, A. Esteve-Nuñez, A. Berná and J. M. Feliu, *Angew. Chem., Int. Ed.*, 2008, **47**, 4874; (*c*) D. R. Lovley, *Environ. Microbiol. Rep.*, 2011, **3**, 27; (*d*) K. P. Nevin, S. A. Hensley, A. E. Franks, Z. M. Summers, J. Ou, T. L. Woodard, O. L. Snoeyenbos-West and D. R. Lovley, *Appl. Environ. Microbiol.*, 2011, **77**, 2882; (*e*) V. Coman, T. Gustavsson, A. Finkelsteinas, C. von Wachenfeldt, C. Haägerhäll and L. Gorton, *J. Am. Chem. Soc.*, 2009, **131**, 16171.

3 (*a*) S. K. Chaudhuri and D. R. Lovley, *Nat. Biotechnol.*, 2003, **21**, 1229; (*b*) D. R. Bond and D. R. Lovley, *Appl. Environ. Microbiol.*, 2003, **69**, 1548; (*c*) D. R. Lovley, *Nat. Rev. Microbiol.*, 2006, **4**, 497.

4 H. Hou, X. Chen, A. W. Thomas, C. Catania, N. D. Kirchhofer, L. E. Garner, A. Han and G. C. Bazan, *Adv. Mater.*, 2013, **25**, 1593.

5 (*a*) X. Xie, G. Yu, N. Liu, Z. Bao, C. S. Criddle and Y. Cui, *Energy Environ. Sci.*, 2012, **5**, 6862; (*b*) X. Xie, L. Hu, M. Pasta, G. F. Wells, D. Kong, C. S. Criddle and Y. Cui, *Nano Lett.*, 2011, **11**, 291.

6 (*a*) K. B. Gregory, D. R. Bond and D. R. Lovley, *Environ. Microbiol.*, 2004, **6**, 596; (*b*) K. B. Gregory and D. R. Lovley, *Environ. Sci. Technol.*, 2005, **39**, 8943; (*c*) N. S. Lewis and D. G. Nocera, *Proc. Natl. Acad. Sci. U. S. A.*, 2006, **103**, 15729; (*d*) D. R. Lovley and K. P. Nevin, *Curr. Opin. Biotechnol.*, 2011, **22**, 441.

7 K. P. Nevin, T. L. Woodard, A. E. Franks, Z. M. Summers and D. R. Lovley, *mBio*, 2010, **1**, e00103.

8 T. Zhang, H. Nie, T. S. Bain, H. Lu, M. Cui, O. L. Snoeyenbos-West, A. E. Franks, K. P. Nevin, T. P. Russell and D. R. Lovley, *Energy Environ. Sci.*, 2013, **6**, 217.

9 (*a*) Y. C. Yong, X. C. Dong, M. B. Chan-Park, H. Song and P. Chen, *ACS Nano*, 2012, **6**, 2394; (*b*) Z. He, J. Liu, Y. Qiao, C. M. Li and T. T. Y. Tan, *Nano Lett.*, 2012, **12**, 4738; (*c*) Y. Qiao, S. J. Bao, C. M. Li, X. Q. Cui, Z. S. Lu and J. Guo, *ACS Nano*, 2008, **2**, 113.

10 (*a*) Z. Luo, Y. Lu, L. A. Somers and A. T. C. Johnson, *J. Am. Chem. Soc.*, 2009, **131**, 898; (*b*) J. Zheng, H. Liu, B. Wu, Y. Guo, T. Wu, G. Yu, Y. Liu and D. Zhu, *Adv. Mater.*, 2011, **23**, 2460.

11 (*a*) B. Gutmann, A. M. Schwan, B. Reichart, C. Gspan, F. Hofer and C. O. Kappe, *Angew. Chem., Int. Ed.*, 2011, **50**, 7636; (*b*) J. Liu, M. Itoh, M. Terada, T. Horikawa and M. Ken-ichi, *Appl. Phys. Lett.*, 2007, **91**, 093101.

12 J. Perelaer, B. J. de Gans and U. S. Schubert, *Adv. Mater.*, 2006, **18**, 2101.

13 (*a*) P. Toneguzzo, G. Viau, O. Acher, F. Fiévet-Vincent and F. Fiévet, *Adv. Mater.*, 1998, **10**, 1032; (*b*) C. M. Watts, X. Liu and W. J. Padilla, *Adv. Mater.*, 2012, **24**, OP98; (*c*) M. Baghbanzadeh, L. Carbone, P. Davide Cozzoli and C. Oliver Kappe, *Angew. Chem., Int. Ed.*, 2011, **50**, 11312.

14 T. Mahmood, M. T. Saddique, A. Naeem, P. Westerhoff, S. Mustafa and A. Alum, *Ind. Eng. Chem. Res.*, 2011, **50**, 10017.

15 M. Kosmulski, *Chemical Properties of Material Surfaces*, Marcel Dekker, Inc., New York, 2001.

16 J. E. Mink, J. P. Rojas, B. E. Logan and M. M. Hussain, *Nano Lett.*, 2012, **12**, 791.

17 (*a*) T. J. Beveridge, *J. Bacteriol.*, 1999, **181**, 4725; (*b*) M. Sára and U. B. Sleytr, *J. Bacteriol.*, 2000, **182**, 859.

18 (*a*) S. A. Cheng and B. E. Logan, *Electrochem. Commun.*, 2007, **9**, 492; (*b*) B. Lai, X. Tang, H. Li, Z. Du, X. Liu and Q. Zhang, *Biosens. Bioelectron.*, 2011, **28**, 373.

19 K. R. Krishnadas, P. R. Sajanlal and T. Pradeep, *J. Phys. Chem. C*, 2011, **115**, 4483.

